7-6

Lung Tumors of Primates and Rodents

Part III

Gerrit W. H. Schepers, M.D., D.Sc.

The materials reviewed include **269** industrially induced human lung cancers and **276** pulmonary neoplasmata, which developed in monkeys. rabbits, guinea pigs and rats after inhnlation exposure or intratracheal injection of **266** chemical substances. The animal tumors developed **in 10,768** experimental subjects, whereas **4,143** control animals, marched tor sex, age arid survival, showed no tumors. In addition to neoplasia, there **wcrc** large numbers of **lesions** that **werc** judged **to** be pre·neoplastic. The morphology of the animal tumors is compared with that of human **tumors** and some homologies **were** identified. **A** tentative explanation of the histogenesis **of** morphological varieties of animal tumors is offered.

MORPHOLOGY OF LUKG TUMORS

In Table 18, a classification is presented of the anatomical features of the tumors observed in the animals of this series of experiments. The Table also lists a few lesions that appear to be tumor precursors. It is fully appreciated that this classification does riot entirely correspond with classificatory schemata that previously have been published by other authors. It is not intended that this classification substitute for other systems. Table **18** is based entirely **on** the histological variables observed in the animals personally studied.

Adenomatoid Carcinomata

The most prevalent tumor was the adenomatoid variety. This term is proposed since the tumor, though invariably malignant, **mimics** the histoarchitecture of the pulmonary adenoma frequently found in mice. The tumor grows marginally and invades the lung without compressing it. There may be central fibrosis, but sometimes the tumor remains epithelial throughout. The adenomatoid tumor was often multifocal when first discovered. This may signify simultaneous carcinogenesis **at** multiple sites, but may also be indicative of early intrapulmonary metastases.

By expanding progressively, **multiple** nodules oftcn werc palpable within excised **lung** tissue. Many tumors lie superficially, **so** that they present 3t the surface (Fig. 6A). Others lie deeper and **are only** scen on section (Fig. 6B). **Tumors** varied in stages of development. Gross tumors oftcn were in juxtaposition to Icsions requiring microscopic demonstration.

Adenomatoid tumors prcscntcd **as** several morphological varieties. The basic lesion appeared to be the acinoid variety in which rougly circular ssccules lined by a **single** layer of epithelium are juxtaposed to **one** another (Fig. **6C).** The cells lining these acini varied **from** low cuboidal to columnar epithelium and sometimes goblet cells predominated. The acini may be empty or may contain desquamated epithelial cells, polymorphonuclear leukocytco or koniophages. hlucopolysaccharidr could dc demonstrated in **some** acini, but not in all. **A** cellular and sometimes **a** fibrous stroma sometimes separated the acini, but often acini **show** minimal non-tumorous material between them.

These relatively bcnign-weming tumors metastasized readily and could be homotransplanted *to* subcutaneous tissue whence dissemination to other organs readily occurred. Metastases occurred unpredictably. Relatively small primary tumors sometimes produced enormous secondary lesions at an early stage. **In** other instances, relatively large and destructive **lung** tumors failed to spread beyond the thorax until very late.

The **most** frequent metastatic site was the kidney (Fig. 6D). These tumors almost invariably located in **the** renal cortex, and by progressive and rapid **enlargement,** bulged through the rcnal capsule. **Thought** was given *to* **the** possibility that such rcnal tumors were primary lesions

TABLE 18. Pulmonary Tumors Experimentally Induced – Animal

A *NEOPLASTIC*	
Histologic Organization	Cytologic Variants
Adenomatoid	
Acinoid	Cuboidal Cell
Papilligeroid	Columnar Cell
Circinoid	Goblet Cell
Mucigeroid	
Epidermoid	
Desquamative	Small Cell
	Large Cell
	Pleomorphic
Multilayered	Squamoid
	Pearl Forming
	Keratinizing
Mesothelioid	Fibroblasts
	Mesothelial Cell
	Endothelial Cell
Lymphomatoid	Lymphocytic
	Reticulocytic
Mixed	Alveologenic
0 PRE-NEOPLASTIC	
Alveolar Epithelialization	Alveologenic
	Bronchiologenic
Bronchiolar Epithelial Plaque Metaplasia	
Granulomatoris	
Lymphoid Hyperplasia	
Pleural Plaque Formation	
Pleural Mesothelialization	

caused by the hemic transportation of the absorbed carcinogen to the renal cortex. There are three reasons for rejecting this hypothesis, namely, (3) no carcinogenic test substance could be demonstrated in the renal tumor; (b) histologically, the renal metastasis closely resembled the pulmonary lesion; (c) renal metastases often occurred during homo-transplant experiments even through the 5th generation (Table 17).

Other common sites of metastases included regional lymph nodes, the adrenals, liver, spleen, brain and even bone.

The next variant of the adenomatoid tumor has been designated papilligeroid. The gross morphology of this tumor is not clearly different from that of the preceding type, but on lung section (Fig. 7A) it could often be noted that this tumor is less clearly defined at the margins, seeming to invade pulmonary parenchyma more irregularly and tending less to bulge out under the pleura.

Histologically, this tumor is cliaracterized by the prevalence of micropapillomata (Fig. 7B). These may project into acini or the papillary growths may branch so widely and irregularly that no acinoid elements are preserved. In most instances. these tumors are non-secretory, so that no mucopolysaccharides could be demonstrated in the spaces around the micro-villi. Some desquamation of superficial cells otcurred in most areas. Often the pedicles of the villi comprised a double epithelial structure with vigorous mitoses in low cuboidal hyperchromatic cells. Occasionally, some papillae were covered with mixtures of cuboidal and columnar cells.

A circinate variant of tumor was observed in some instances (Fig. 7C). Histologically, this tumor may bc intermediate between the acinoid and papilligeroid tumors. Characteristically, several plications of single layered cpithclium were found as coiled sheets within acinoid spaces. These coils may represent modified papilli or may be the result of duplication of the epithelial lining of acinoid lesions. That this variant of tumor architecture was not merely an isolated, fortuitous genetic aberration was evidcrit when the identical pattern was recapitulated in rcnal metastases of second generation homotransplants (Fig. 7D).

A fourth variant of the adenomatoid neoplasm of this series of experiments has been designated mucigeroid. These tumors were macroscopically identifiable (Fig. 8A). The naked eye appearance of tumors that reached the lung surface was that of a bluish grey glistening cyst which conformed with the lung contours instead of

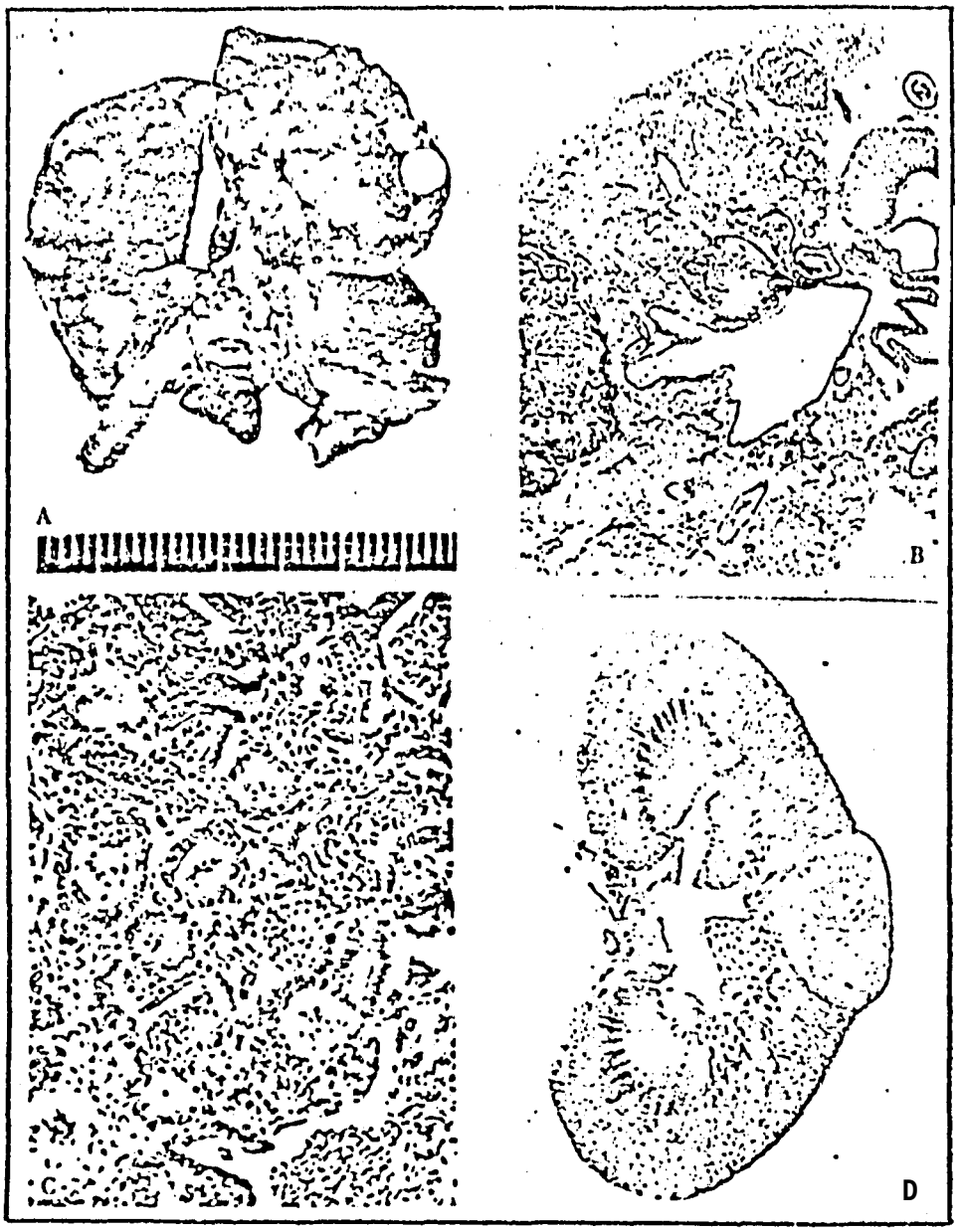

FIGURE 6. Adenomatoid carcinoma induced by inhalation of beryllium sulphate (12 γ/ft³): Rats

A. Gross Morphology of Lung: Continirour exposure for 14 months. Multiple tumors are discernable;

B. Coronal Section of Lung: Three (3) discrete tumors are present in a single plane and a lymph node contains metastatic tumor. Exposure for 6 months plus normal air 6 months;

C. Acinoid Histology: 6 months $BeSO_4$ followed by 8 months normal air. Neoplasm consists of vesicles lined by polyploid cuboidal epithelial cells;

D. Metastatic Renal Tumor: Primary lung tumor found after 15 months was homotransplanted to subcutaneous tissue through two (2) generations. The renal metastasis was histologically identical to the primary lung tumor.

bulging through the pleura as did other more solid tumors. On lung section, the tumors could easily be overlooked since they did not possess the cellularity of the preceding lesions (Fig. 8B). The "cysts" did not drain empty when cut, but resembled a jelly held together in epithelial saccules and supported by delicate stromal elements: Histologically, the lesion is of the acinoid vsriety, but the saccules are much larger and this may be due to distension by accumulated mucopolysaccharide. The ssccules arc lined by alternating zones of cuboidal, columnar and goblet ccll epithelium. Along the edges of the mucus-filled spaces, small circuisr epithelium-lined structures represent the actively growing elements of the tumor. These marginal protrusions provide a dark edging to the cysts as seen in gross section.

At first these mucigeroid tumors were viewed as relatively benign lcsions or as representing an end stage of a previously more active lesion. On homotransplantation, this concept was dispelled. The tumors readily reproduced in the host tissue and disxminsted diffusely. The mucigerous propensity tended to be lost aftcr one or two transplantations and the tumor became perpetuatcd as a highly cellular lesion in which some attempt at acinus formation persisted (Fig. 8D).

Epidermoid Carcinomata

The next group of tumors has been designated epidermoid. They are cliaracterized by epithelia which tcnd to grow in multiple layers rather than as single sheets of ccIls plicated to form acini or papilli as in the adcnornatoid tumors. Morphologically. all these tumors tended to be relatively solid and circumscribed (Fig. 9A), brit *two* basic histological types were differentiated namely, desquamative and multilayered.

The desquamative variant appears to represent a transition from tlic acinoid variety. Histologically, a

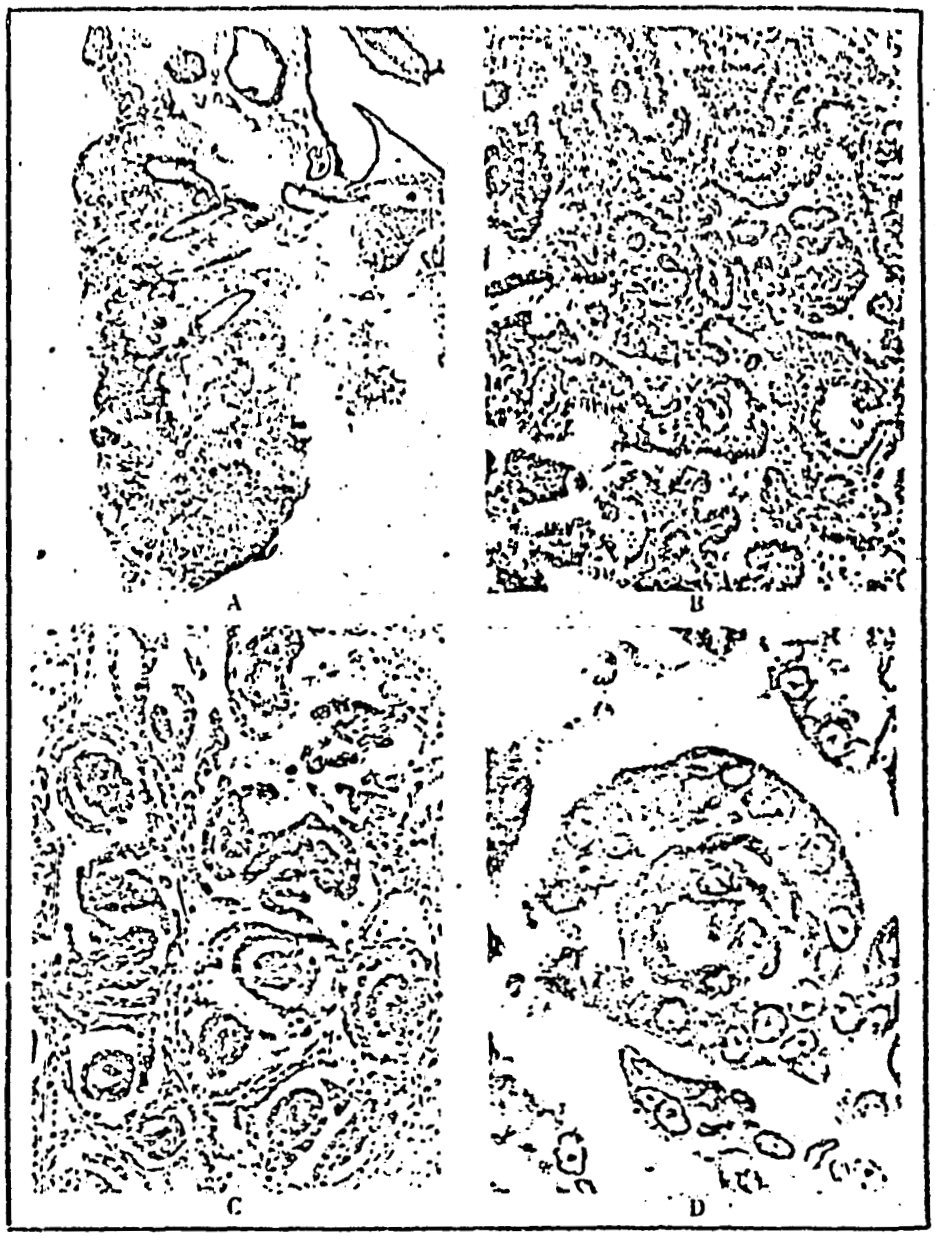

FIGURE 7. Adenomatoid carcinoma: Inhalation exposure to beryllium aerosols: Rats

A. Coronal Section of Lung: Inhalation *oi.* $BeSO_4$ (12 7/11') for 6 months followed by quartz dust (50 mp/ft³) for 6 months. Multiple regular tumors invade lung parenchyma.

B. Papilligeroid Histology: Inhalation exposure to BeF_2 (1.36 γ/ft³) lor 14 months. Tumor consists of papillary projections of hyperchromatic cuboidal neoplastic cells.

C. Circinoid Histology: Inhalation of $BeSO_4$ (12 γ/ft³) for 1 I months. Coiled sheets of tumor epithelium lie within epithelialized acini.

D. Renal Metastasis: The circinoid histologic pattern persists in a metastasis 10 the host kidney after 1st generation subcutaneous homotransplant of the tumor shown in Ft 7C.

vesicular pattern could usually be made out, but the tumor tends to be almost solidly cellular. The acini are filled with cells that hive desquamated from the proliferating epithelium (Fig. 9B). The germinal epithelium may remain denuded. It may also heap up into cellular villi, so that some parts of the epithelium are multilayered (Fig. 9C). Mitosis continues in the desquamated cells or in cells adhering to the basal layer before desquamation (Fig. 9D). The cells vary in size and shape. In some tumors, they arc predominatingly small. In others, most of the desquamated cells are relatively large. Sometimes cell types are mixed and this pleomorphism may include multinucleated neoplastic giant cells.

In the second variant of the epidermoid tumor, the epithelium is regularly multilaminated or stratified. Again, these tumors tend to be almost solidly cellular and form discrete nodules (Fig. 10A). In the simplest variety the epithelial layers arc reduplicated, so that the tumor presents a highly cellular appearance (Fie. 10B). There may be littlc differentiation between the cells or there may bc abortive stages in the establishment of transitional, pseudostratified and stratified epithelium (Fig. 10C and 10D). The component cclls of this multilaycrcd epithelium appear to adhcrc either to the basement membrane by means of delicate ccll pedicles, or are joined together by intercellular bridges. Acanthosis is, however, not a regularly observed feature.

The multilayered epidermoid tumor includes a quite prevalent squamoid variant. These tumors tend to grow large locally and are dense or hard on palpation (Fig. 11A). The abundant, but usually no erythrocytes were discernible the form of plaques of. keratin-dense flattcned cclls. At this stage, the squamoid cclls still contain hyperchromatic nutlci showing prevalent and atypical mitosis (Fig. I In). There is a tendency to whorling of the epithelial squamous cell: and typical epithelial pearls were often the rcsult (Fig. 11C). In other squamoid tumors, keratinization predominates. The keratin is laid

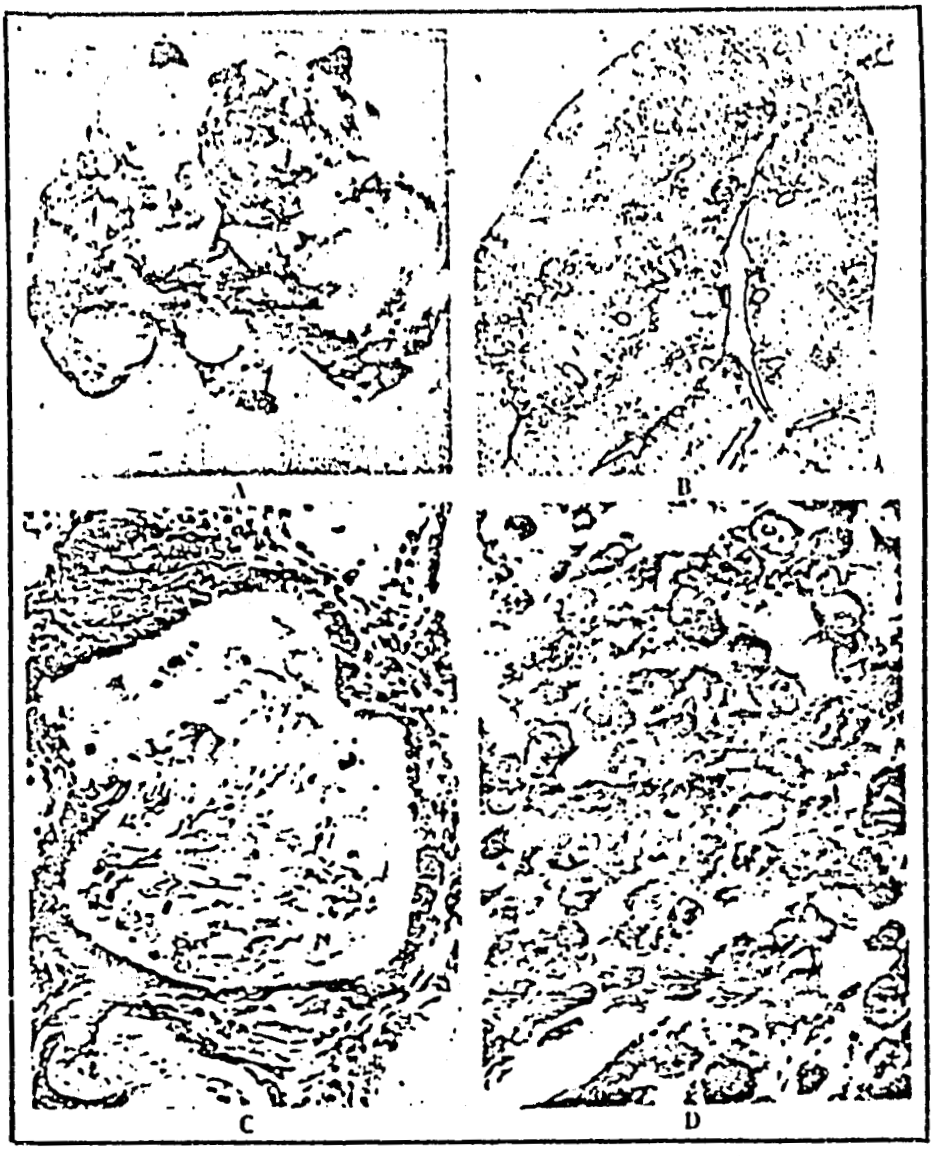

FIGURE 8. Mucigeroid pulmonary adenocarcinoma: Inhalation exposure to $BESO_4$ (12 γ/ft³): Rats

A. Gross Morphology:
After 12 months $BeSO_4$ followed by 6 months normal air. Multiple cyst-like tumors discernable under pleura;

B. Coronal Section:
$BeSO_4$ 6 months plus 10 months normal air. Multiple parabronchial amorphous lesions are edged by dark staining cells:

C. Mucigeroid Histology:
Fringe zone of lesion shown in 8B. The tumor consists of vigorously growing acini which partially fill with mucinous material and desquamated cells;

D. Second Generation Homotransplant:
Hepatic metastasis of tumor shown in 8B and C. Abortive acini are recreated among wildly proliferating neoplastic cells.

FIGURE 9. Epidermoid pulmonary carcinoma with transitional desquamative histology

A. Coronal Section:
Rat Lung: Inhalation of BeSO, (12 γ/ft³) for 6 months followed by normal air for 10 months. Highly cellular pulmonary tumor and metastasis *to* regional lymph node;

B. Desquamative Type:
Rat Lung: Exposure as for 9A. The histology is transitional between acinoid adenocarcinoma and epidermoid carcinoma. In some acini, all layers of cells have desquamated. In others, only superficial cells have dropped off;

C. Pseudo-Stratified Histology:
Rabbit Lung Zinc manganese beryllium silicate (0.74 mg/ft³) for *9* months plus normal air for *6* months. Epithelial cells are piled several layers thick at some locations, but each cell reaches basement membrane;

D. Mululayered Epithelium:
Rat Lung: Beryllium phosphate (0.11 mg/ft³) for 6 months plus normal air for 6 months. Note atypical mitosis within the epithelial layers. Stratification has not developed.

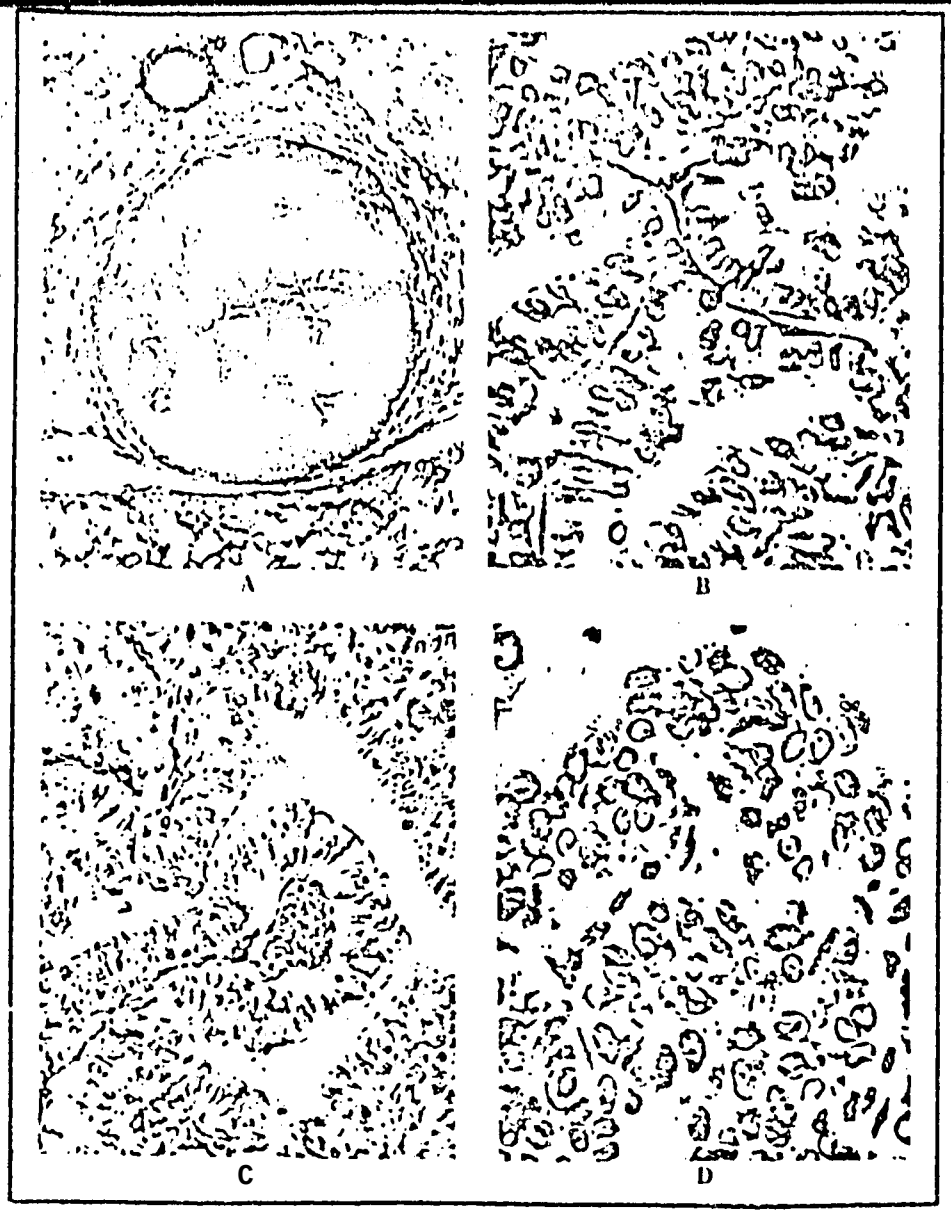

FIGURE 10. Epidermoid pulmonary carcinoma with plicated histology

A Tumor Nodule Gross Section: Guintn Pig Lung: Inhalation exposure *to* coal dust for 10 months followed by normal air for 32 months. Tumor tissue stains intensely because of high cellular content;

B. Multilaminated Epithdium: Monkey Lung: Inhalation *of* $BeHPO_4$ (373 γ/ft^3) for ten (10) days followed by normal air for 82 days. Acinoid pattern is preserved, but several layers of epithelium are present throughout;

C. Pseudo-Stratified Epithelium: Guinea Pig Lung: Hematite dust for 42 months followed by normal air for 9 months. Although cell nuclei are at different levels, the cytoplasm appears to reach the basement membrane in most cases;

D. Stratified Epithelium: Rat Lung: $BeSO_4$ 10 months plus normal air 10 months. The tumor trabeculae are composed of multiple cell layers with apparent stratified organization.

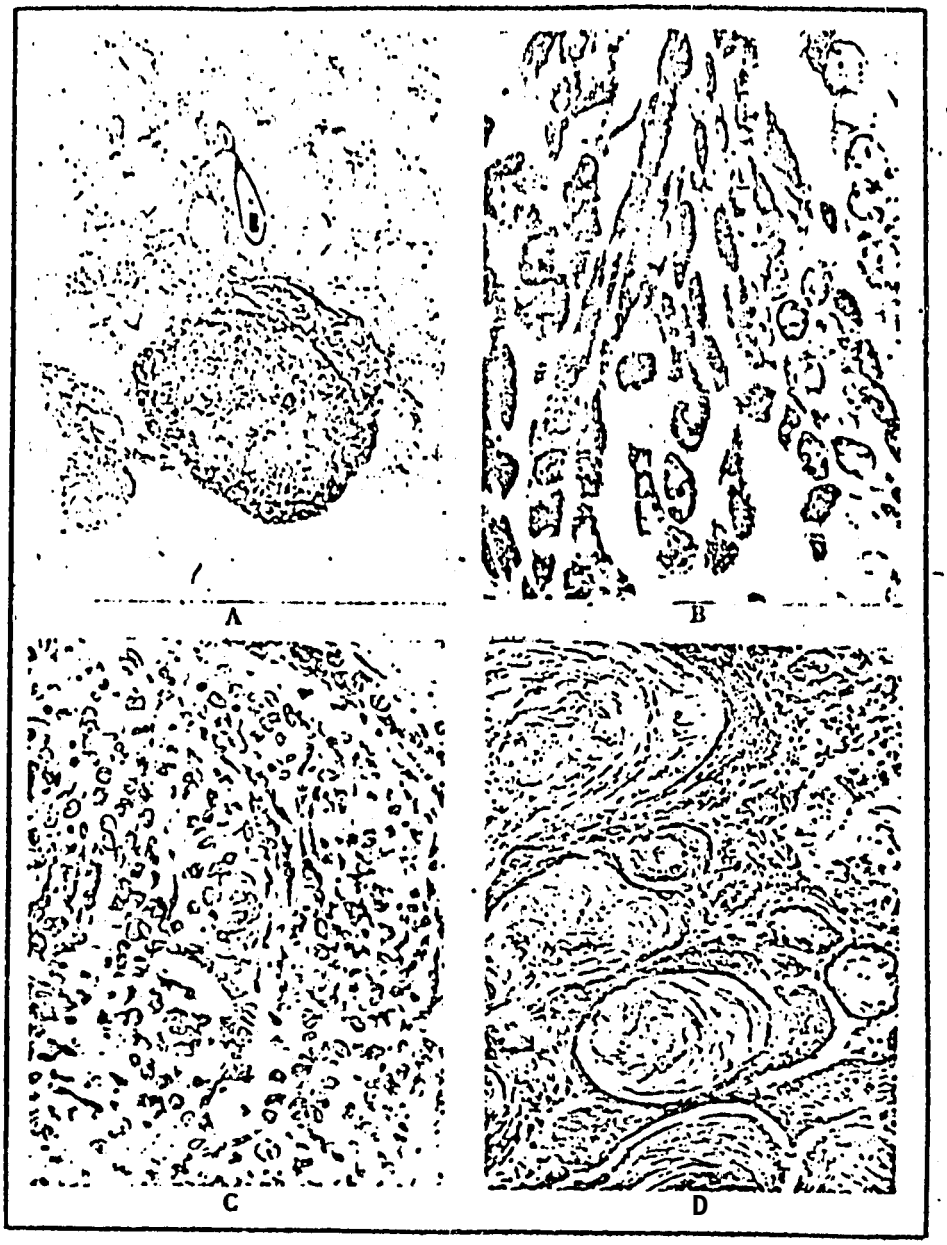

FIGURE 11. Epidermoid pulmonary carcinoma with squamoid histology

A. Tumor Nodule: Gross Section Rat Lung: $BeSO_4$ (12 γ/ft³) for 6 months then Fe_2O_3 (10 mg/ft³) for 12months followcd by normal air for 1 month. One of several discrete tumors in these lungs;

B. Squamoid Histology: Guinea Pig Lung: BeO (1.4 γ/ft³) for 12 months. Note flattening of surface cells of tumor epithelium, which *also* shows pe sistent mitosis at a distance from the basal layer;

C. Pearl Formation: Monkey Lung: $BeHPO_4$ (373 γ/ft³) for 10 days plus normal air for 82 days. Some of the irregularly growing neoplastic cells are whorled lo create an epithelial pearl;

D. Keratinization: Rat Lung: $BeSO_4$ for IS months. Squamoid carcinoma predominates and acinoid spaces are Tiled with layers of keratin.

FIGURE 12 Pulmonary mesothelioid tumor

A. Gross Morphology:
Rat Lung: BeSO, for 12 months plus normal air for 6 months. The massive projection from the surface is the mesotheliod tumor. Other lesions are In — .. pulmonary neoplasmata;

B. Gross Section:
Rat Lung: $BeSO_4$ for 6 months then quartz dust for 10 months. Tumor is attached to lung by means of a sessile pedicle;

C Mesothelioid Histology:
Rat Lung: $BeSO_4$ for 6 months plus normal air for 12 months. Densely cellular pleural tumor metastasized widely;

D. Homotransplant Histology:
Rat Spleen: Second generation subcutaneous homotransplant metastasized to spleen. Tumor consists of cellular trabeculae without intervening stroma or vascular elements

down in multiple laminae and mostly seems to represent compressed hyperkeratinized epithelial cells. In some cases, no vestiges of cell structure could be identified in the keratinized zones.

Mesothelioid Tumor

. This tumor generally was readily identifiable because it projected from the surface of the lung in an obstrusive manner (Fig. 12A). On section, the continuity of the tumor with the lung could be demonstrated (Fig. 12B). This illustration demonstrates well that the tumor is superficial to the plane of lung and there is no parenchymal lesion in the lung opposite the point of insertion of the sessile tumor pedicle. The tumor presses into the lung, which conforms to the shape of the tumor.

Most of these mesothelioid tumors appear to start as solidly cellular neoplastic growths attached to the outer surface of the lung (Fig. 12C). As they grow larger. further histological organization takes place, a pedicle forms and stromal elements may appear.' The cellular tumors appeared to be highly malignant, metastasized early and remotely and could be readily transplanted. When regrown in a host organ. the mesothelioid tumor' formed solid cell masses or irregular cellular trabeculae without stroma or vascular elements (Fig. 12D).

In some instances,' the mesothelioid tumors were highly vascularized and endothelial proliferation' occurred along with the mesothelial proliferation. Capillary loops were abundant, but usually no erythrocytes were discernable suggesting that thex capillaries are derived from pleural lymphatics rather than small blood vessels. In other instances, the mesothelial tumors werc composed mainly of proliferating fibroblasts with some interstitial infiltration of lymphocytes and histiocytes. A final subvariant of the mesothelioid tumor is charac-'terized by the presence of acinar patterns. This tumor is indistinguishable from the adenomatoid intrapulmonary tumors previously described and probably represents a cortical pulmonary tumor which has eroded through the pleura. This tumor may. thercforc, be designated the alveologenic or pscudomeso thelioid tumor.

FIGURE 13. Lymphomatoid lung tumors

A. Gross Section:
Rat Lung: $BeSO_4$ (12 γ/ft³) for 6 months plus chrysotile (226 mp/ft³) for 6 months Three (3) tumors in this plane of section

B. Lymph Node Metastases:
Rat Lung: BeO (1.4mg/ft³) for 6 months then quartz dust (10 mp/ft³) for 8 months. The lymph node metastases of a primary lung tumor predominate;

C. Tumor Cytology:
Rat Lung: Same exposure as 13A. The tumors consisted throughout of such hyperchromatic anaplastic cells;

D. Pleomorphic Cytology:
Rat Lung: $BeSO_4$ for 6 months plus normal air 10 months. Multinucleated giant cells are present.

Lymphomatoid Tumor

Some of the experimental animals displayed lymphomatoid tumors. That these tumors originated within the lung itself was well demonstrated in several instances when no extrapulmonary counterparts were demonstrable (Fig. 13A). More usually the pulmonary tumor rapidly involved the regional thoracic lymph nodes which enlarged to prodigious proportions (Fig. 13B). The tumor also disseminated to both extra thoracic lymph nodes and to other organs. Cytologically, the tumor consists of two varieties. The first has rather uniform cells with minimal cytoplasm and large hyperchromatic nuclei. These cells resemble lymphocytes or plasma cells (Fig. 13C). The second variety is comprised of larger cells with more vesicular nuclei and cytoplasm. Sometimes giant multinucleated cells were present (Fig. 13D). On applying silver stains. a delicate reticular stromal meshwork could generally be demonstrated.

Mixed Tumors

in several instances, moie than one histological type of tumor was demonstrable in the same set of lungs. In some animals the histology of tumor metastases also was significantly different from that of the primary lung tumor. Thus, when the predominating pulmonary tumor was a squamoid carcinoma, the renal or hepatic metastasis was either a medullary or an acinoid type of lesion. This pleopotentialism of the tumors of this series was again demonstrated by the frequency with which tumors changed in histology as they progressed through successive gencratiqns or metastasized to different organs during homo-transplant experiments (Table 17). The inference appears justified that the detailed tumor

histology may be influenced by factors other than the extraneously applied carcinogenic stimulus.

Preneoplastic Lesions

Every morphological stage of transition from normal lung tissue to true neoplasia could be identified in this series of experimental animals.

Epithelialization of alveolar surfaces was the most obtrusive feature. Several varieties were observed. The alveologenic lesion commenced in isolation within alveoli remote from bronchiolar structures. Sometimes these lesions were most prevalent within subpleural alveoli. In the earliest phases, isolated sectors of alveolar surfaces displayed epithelial plaques with polyploid hyperchromatic cells (Fig. 14A). At later developmental stages, individual alveoli were observed to be completely epithelialized. In the next step, papillary projections into the epithelialized spaces could be observed (Fig. 14B). It takes little imagination to deduce how the acinoid and papilligeroid tumors could derive from these epithelialized vesicles.

That the epidermoid tumor is not merely a complication of the preceding structures is revealed by the discovery of primordial plaques of multilayered proliferating centers at discrete parenchymal locations. In some instances, the plaque remained clearly cellular and this may be the precursor of a multilayered epidermoid tumor (Fig. 14C). In other instances, squamoid plaques could be discerned on the surfaces of alveolar vesicles where no other cellular aberrations had yet developed (Fig. 14D). Perhaps these squamous plaques are the way some squamoid carcinomata start.

Epithelialization of alveolar spaces may also derive from bronchiolar epithelium (Fig. 15A). Such epithelialized areas lie either to one side of, or surround a bronchiole or alveolar of epithelialization and neoplastigenesis. This phenomenon may be goblet cells. Mucus and cellular detritus may also accumulate within the distorted parabronchiolar alveoli. It seems likely that this type of lesion may be the precursor of the mucigeroid variety of adenomatoid carcinoma.

Very rarely there were preneoplastic epithelial changes within the bronchioles. Sometimes these were relatively diffuse (Fig. 15B) and at other times there was focal proliferation only (Fig. 15C). Since no endobronchial tumors were observed in this series of experiments, it seems possible that neoplasia, originating from a group of cells within a sheet of bronchial epithelium, may quickly metastasize to alveolar regions and proliferate there instead of at the original site (Fig. 15D).

Pleural plaque formation may be one variety of precursor to the mesothelioid tumor. Most plaques consisted of local accumulations of fibroblasts and lymphogenic cells which spread laterally over the surface of the pleura, retaining a sessile point of attachment to the pleura. Sometimes the plaque has no lesion opposite it in the lung (Fig. 16A). At other times, the plaque appears to be an extension of a subcortical fibrocellular lesion (Fig. 16B). Pleural tumors may also derive from neoplastic change of the mesothelial epithelium. Under the stimulus of some inhaled chemical agents, the mesothelium proliferates to form a continuous or discontinuous pseudocuboidal epithelium (Fig. 16C). Occasional foci of reduplication and papilloma formation in this mesothelium may be the immediate precursor of the tumor. These mesothelial cells also desquamate and could be observed in aspirates of pleural fluid. Since parenchymal tumors often arose in tissue immediately subjacent to the pleura, the demonstration of ulceration of such a tumor through the pleura seems pertinent (Fig. 16D). The plaque, which is forming where the tumor is eroding through, may be designated a malignant plaque.

The pulmonary granuloma may also represent a precursor to carcinogenesis. The graphs of Fig. 3 illustrate how the evolution of granulomatosis runs parallel to the emergence of epithelialization and neoplasiogenesis. This phenomenon occurred not only with BeO, but also during experiments with $BeSO_4$, BeF_2 and $ZnMnBeSiO_4$.

The typical granuloma contains several cellular elements which may embryonate to tuniors. Some granulomata are composed mainly of large cells with vesicular nuclei which may derive from alveolar β cells (Fig. 17A). It is possible that neoplastic transformation of these cells may account for the squamoid tumors which were sometimes seen *to* develop on the basis of a granuloma (Fig. 17B). Other granulomata are composed mainly of plasma cells and lymphocytes (Fig. 17C). It seems likely that these cells could represent the precursors of lymphomatoid tumors of the type represented in Fig. 13C. Some granulomata also become covered by a cuboidal epithelium (Fig. 17D). This layer may derive from alveolar β cells. In a sense, this arrangement merely represents alveolar epithelialization in another anatomical location and may have the same relationship to lung tumors as has the epithelialization previously discussed.

HOMOLOGIES

The aforementioned series of tracheal injections and inhalation experiments were designed to cast light on the biological potentials of industrial substances. To a large extent. this objective was achieved, including demonstration of the selective carcinogenicity of certain materials. A few features, however, remain unclarified. These concern the comparative morphology of human and animal lung cancers.

Human lung neoplasmata may be classified as in Table 19. At first glance there appears to be little resemblance to the classification of the tumors induced in monkeys, rabbits, guinea pigs and rats (Table 18).

TABLE 19. Pulmonary Neoplasia — Human

Origin	Benign	Malignant
Epithelioid		
Bronchial	Papilloma	Epidermoid (squamous) carcinoma
	Atlcnoma	Adenocarcinoma
	"Carcinoid"	Acinary
	Oncocytic	Papillary
	Cylindroid	Mucoid
Parenchymal	Bronchiolar metaplasia	Anaplastic carcinoma
		Oat, Round. Small.
		Spindle, Giant Cell types
	Atypical proliferation	Carcinosarcoma
Mesodermoid		
Bronchial	Fibroma, Lipoma	Fibrosarcoma
	Chondroma, Osteoma	Osteocondrosarcoma
	Myoma	Leiomyosarcoma
	Neuroma	Neuroblastoma
Parenchymal	Hemangioma (capillary, cavernous, endothelioma)	Hemangiosarcoma
		Malignant Lymphoma
		Hodgkins Sarcoma
Congenital	Hamartoma	Teratosarcoma
	Teratoma	
Pleural		
Mesothelioma	Fibroid plaque	Fibrosarcoma
	Cellular plaque	Mesotheliosarcoma .
		Endotheliosarcoma

So morphological ~ - ' ~ m u between benignity and maligrity of the anrnal rumors could be established. Most pathologists distinguish, with reasonable confidence, between benign and malignant neoplasms of the human lung. For the animal lesions this was not possible. Tumors with quite simple histological characteristics, and lacking the cytological criteria of human malignancy, often proved highly invasive, metastasized widely and could be transplanted through many generations. On' the ip of experimentally induced lesions designated .. -neoplastic" probably were "benign" and would perhaps represent animal homologues of human benign tumors.

A second mjor difference between the animal and the human tumors lies in the paucity of mesodermoid lesions in the former. In animals the only lcsions that matched with similar lesions in man were the lymphoma. toid and mesothelioid tumors.

The third major difference lies in the fact that the animal tumors arose in the pulmonary parenchyma, whereas, primary human lung tumors arc frequently located in the bronchi. One explanation for chis difference may be based on as yet poorly defined anatomical homologies between the human and animal lung. It may be possible that the portions of the human bronchial tract, which are the sites where lung cancer usually manifests itself *(Fig.* 18A), correspond to structures which are designated bronchioles, alveolar ducts and peri- or parabronchiolar alveoli in animals (Fig. 18B). An alternative explanation may be that human lung tumors are seldom seen at the early stage possible in animals. Perhaps in man the earliest Icsion is neccsrarily overlooked. The bronchial carcinoma which the pathologist identifies, at a late stage in the cvolutiori of the disease, really may bc a bronchid lymphatic metastasis which grows more rapidly than and obscures a primary parenchymal tumor. In many cases of conventional bronchial cancer, a condition known as "cancerous pneumonia" is seen (Fig. 18C). The presence of neoplastic cells on the alveolar surfaces usually is presumed to be due to aspiration and secondary implantation of bronchia! cancerous cells. However, in these cases there frequently are completely epithelialized alveoli closely resembling the alveolar adenomatoid neoplasm of animals. The possibility must be considered that in some cases at least there alveolar neoplastic cells represent the original tumor, whereas, the bronchial Icsion represents a metasta .. Identical lesions were observed in experimental animals (Fig. 18D) in which no bronchial neoplasia was present *to* create a possibility of retrograde implantation of rumor ccll s on *the* alveolar surfaces.

Most human lung tumors which historically have provided the "type' morphologic patterns from which existing classifications were construed, derived from rclativcly old human subjects. By contract. the experimentally induccd animal tumors reviewed in this account developed relatively early within the life span of

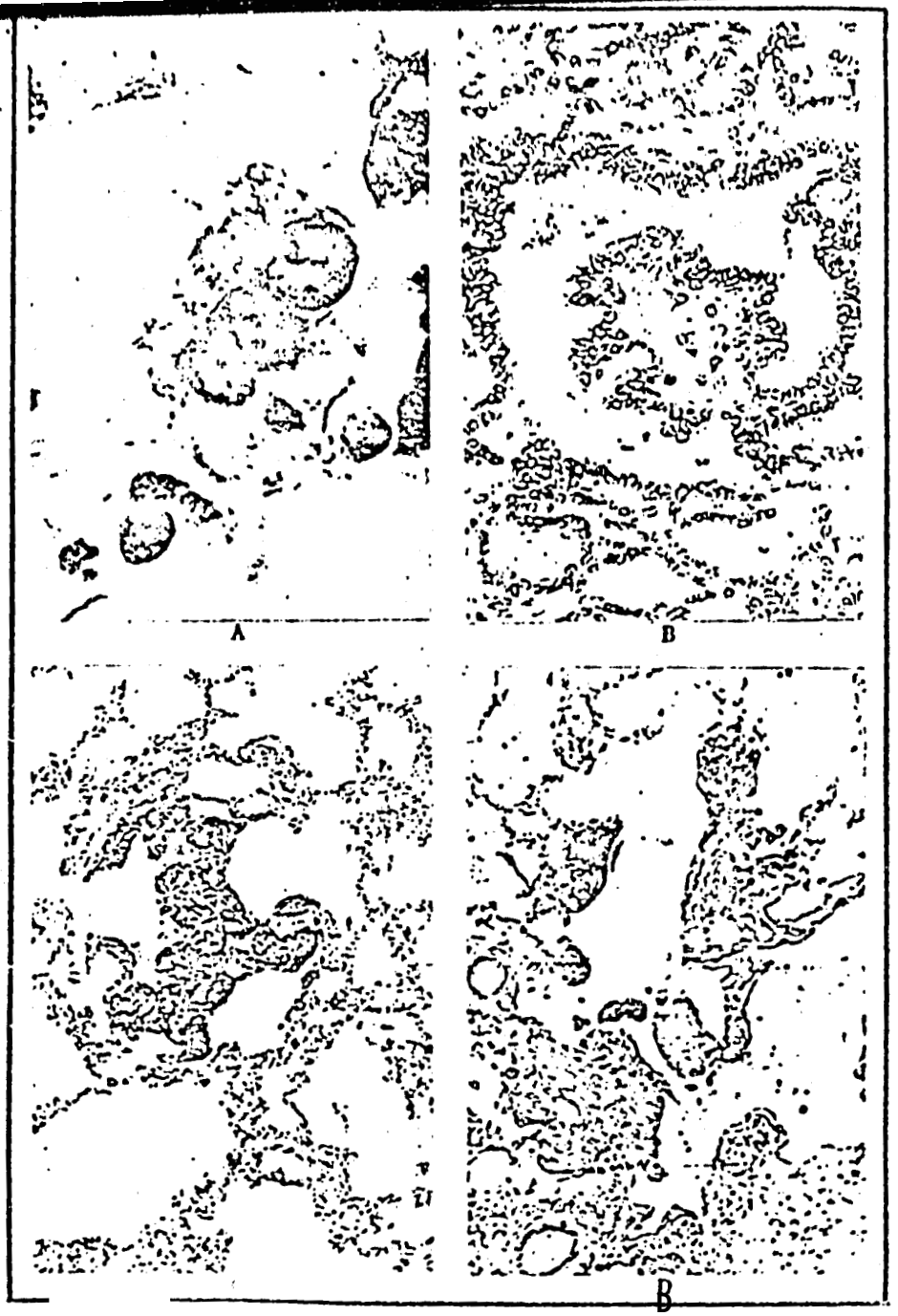

FIGURE 14. Preneoplastic alveologenic epithelialization

A Isolated Cuboidal Cells:
Rat **Lung:** Inhalation **exposure to $BeSO_4$ (12 γ/ft³) for** 6 months. Dyskaryotic **cells** alternate **with** normal septal cells;

B Completely Epithelialized Alveolus:
Guinea Pig Lung: Flux calcined diatomite (1 mg/ft³) for 12 months. Illustrates complete coverage of alveolar spaces **with** low cuboidal epithelium and **incipient** papilla formation:

C. Epidermoid Epithelialization:
Rabbit Lung: $ZnMnBeSiO_4$ **for 6** monlhr plus normal **air for** 3 months. Isolated parenchymal focus with proliferated multilaminated **alveolar** epithelium;

D. Squamoid **Plaque:**
Monkey Lung: BeF_2 **for** 1 nionth **plus** normal air for **2** months. Squamous epithelium has foully replaced alveolar and ductal epithelium.

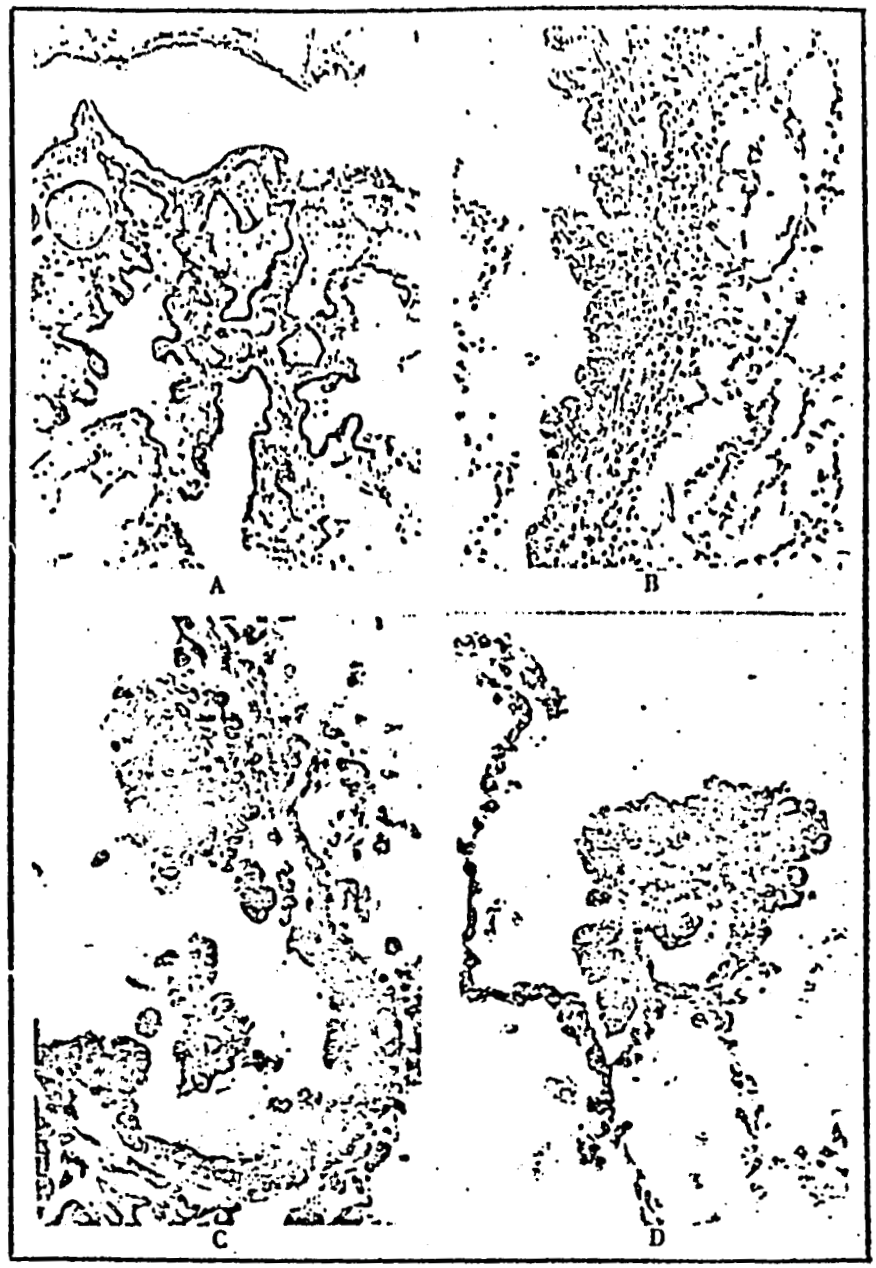

FIGURE 15. Bronchiologenic Epithelial Metaplasia

A. Peribronchial Epithelialization: Rat Lung: Welding fume exposure for 6 months. Extension of bronchiolar epithelium into adjacent alveolar spaces:

B. Bronchial Metaplasia: Guinea Pig Lung: Inhalation for 21 months of on aerosolized mixture of particulate tungsten carbide 75% and cobalt metal 25%. The hyperplastic epithelium has Conned micropapilli or rugae, some of which are ulcerating and desquamating cells;

C. Bronchiolar Micropapillosis: Guinea hg Lung: Inhalation of glass wool dust for 42 months. Local proliferation of bronchiolar epithelium forms a sessile micropapilloma. Glass spicule is discernible);

D. Bronchiologenic Epithelialization: Guinea Pig Lung: Same animal as 15C, Proliferating cluster of epithelial cells may represent transplanted bronchiolar papilloma cells or may represent independent local alveologenic epithelialization.

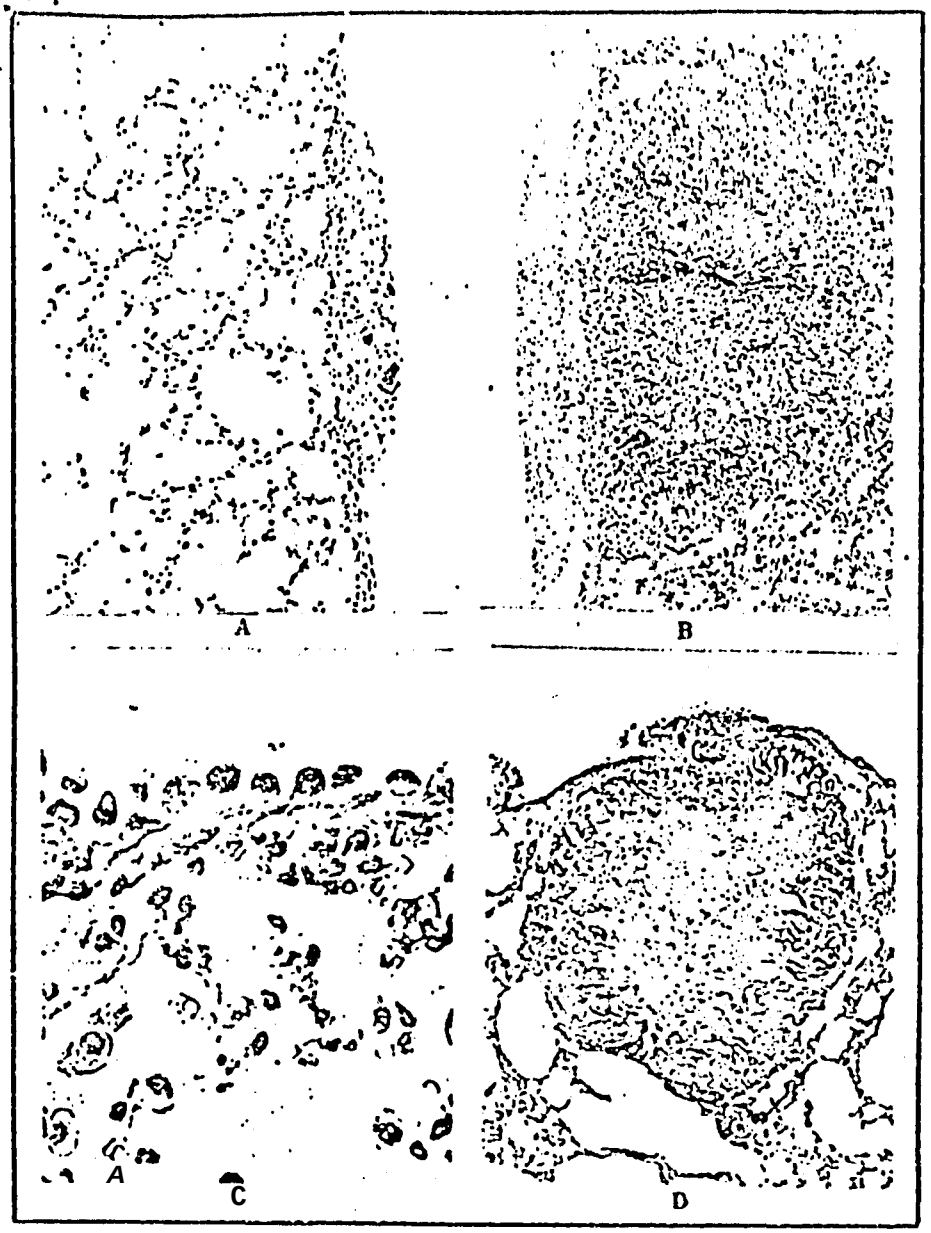

FIGURE 16. Precursors of pleural mesothelioid tumors

A Pleural Plaque:
Guinea Pig Lung: 12 months inhalation exposure to an aerosol of particulate mixed rare *earth* oxides;

B Subpleural Lesion:
Guinea Pig Lung: 12 months inhalation exposure to aerosolized particulate tungsten carbide. The lesion has permeated the pleura and has spread over the surface to form a plaque;

C Pleural Mesothelialization:
Rat Lung: BeF_2 ($1.36\ \gamma/ft^3$) for 6 months followed by normal air for 3 months. Cuboidal cells derive from pleural mesothelium;

D. Erosion of Tumor Through Pleura:
Rat Lung: Pulmonary metastasis from a subcutaneous homotransplant has eroded through the pleura to form a neoplastic pseudo plaque.

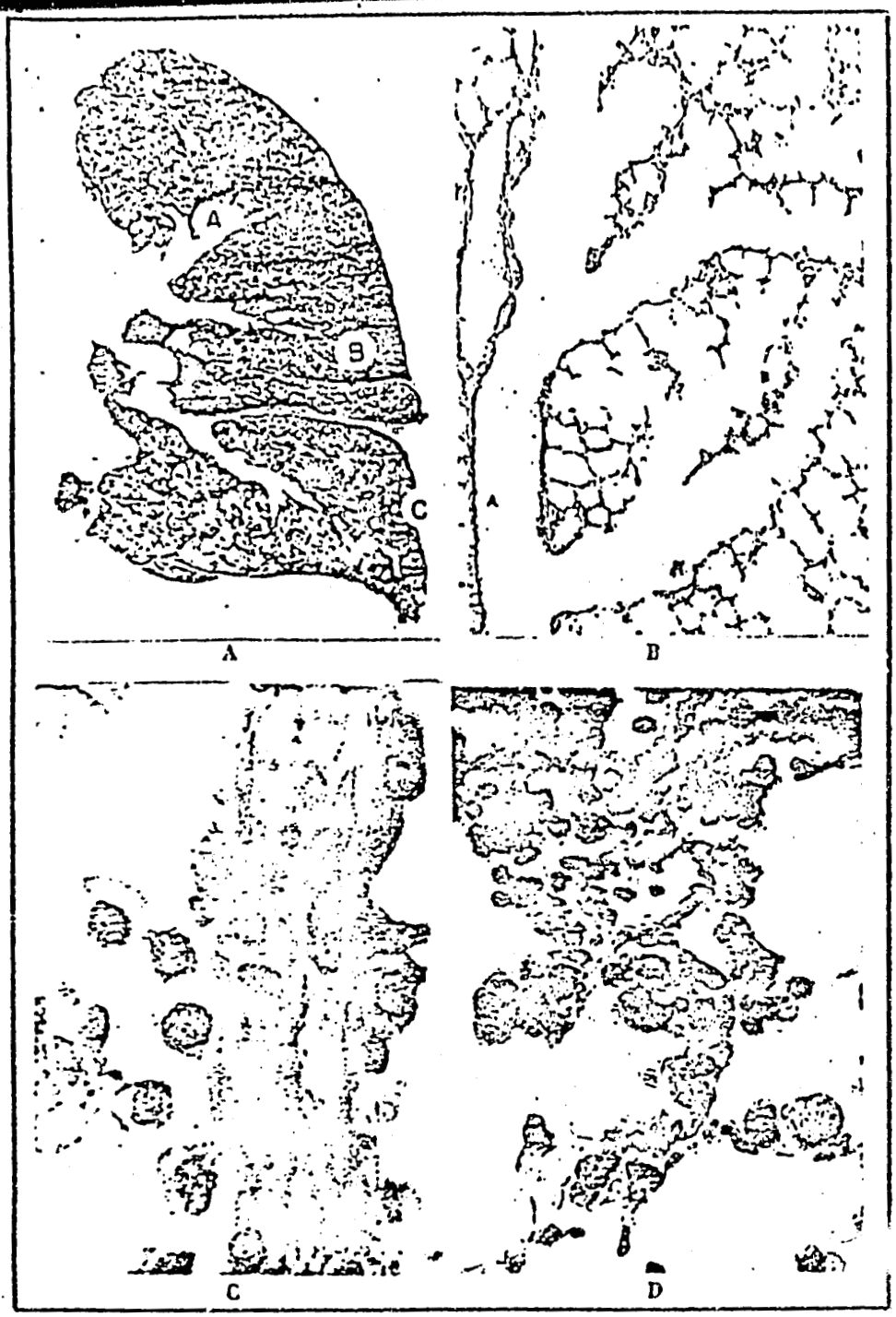

FIGURE 18. Homologies between humanand animal lung tumors

A. Human Respirator). Tract: Coronal section of human lung prepared by Gough technique demonstrating three (3) most common locations of site of origin of tumors, namely, bronchus (a), lung parenchymaand, pleura

B. (c)imal Respiratory Passages:
Microphotograph of guinea pig lung showing bronchioles, alveolar ducts and acini. In the present wries of experiments, tumors were not observed in the bronchi (a) or bronchioles, but were confined b lung par.. enchyma (b);

C. Cancerous Pneumonia:
Human lung showing neoplastic cells attached to surfaces of alveolar septa;

D. Neoplastic Epithelialization:
Rat lung showing neoplastic cells attached to and perhaps arising in situ from alveolar septal cells.

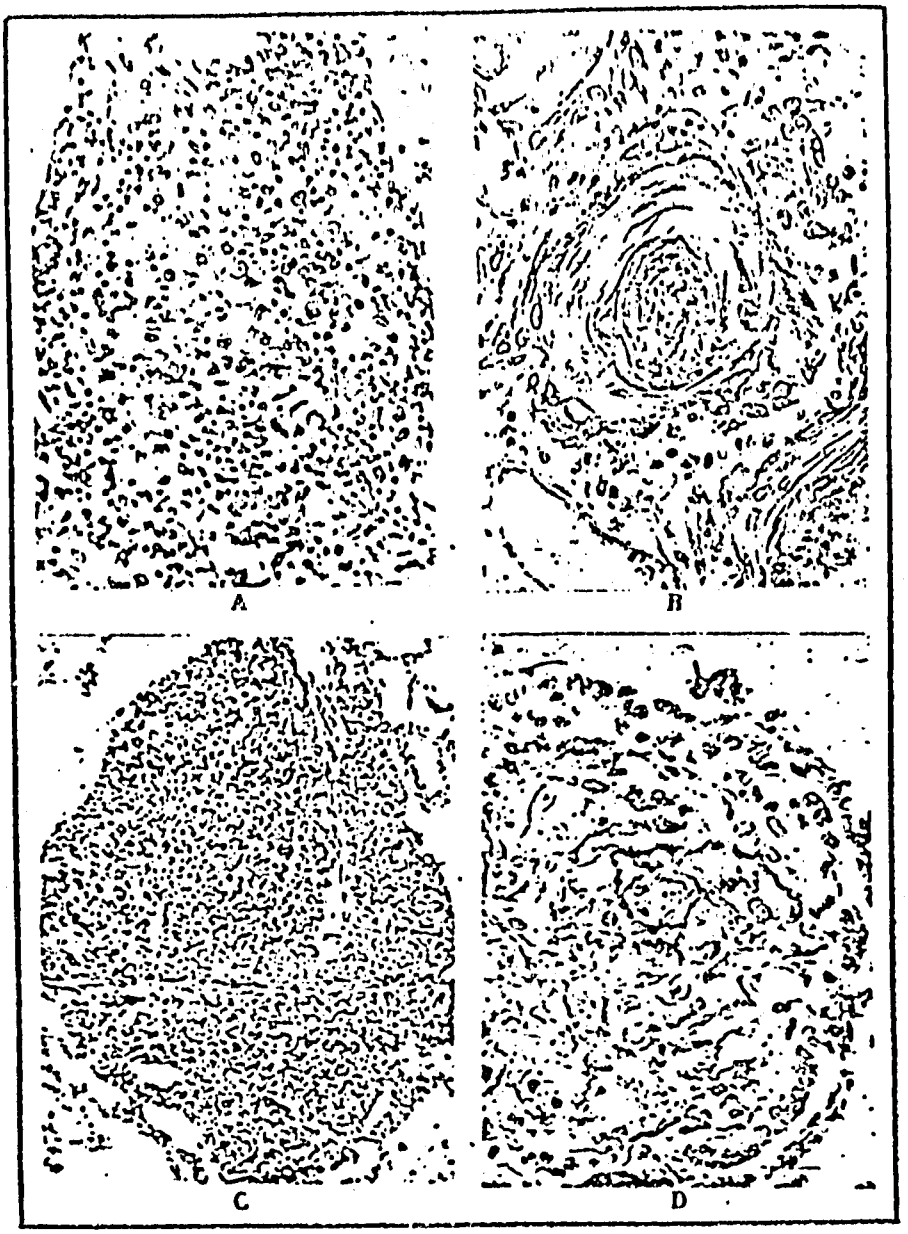

FIGURE 17. Pulmonary granulomata as precursors of tumors

A. Macrocellular Granuloma:
Monkey Lung: Inhalation of $BeHPO_4$ (373 γ/ft^3) for 10 days followed by normal air for 82 days. The predominating cells are large, with vesicular nuclei and may represent alveolar β cells:

b. Squamoid Derivative of Granuloma:
Rat Lung: Inhalation of BeSO, for 10 months then Fe_2O_3 for 6 months followed by normal air for 3 months. The squamoid cells may derive from the β cells of Fig. 17A;

C. Microcellular Granuloma:
Guinea Pig Lung: Inhalation of BeO (.72 mg/ft³) for 8 months then normal air for 3 months. Predominating cells are plasmacytes and lymphocytes:

D. Epithelialized Granuloma:
Rabbit Lung: Inhalation of silicic acid mist for 6 months then normal air for 3 months. Core of granuloma consists of β cells and fibroblasts. Over the surface of the granuloma there is a continuum of cuboidal epithelial cells.

TABLE 20. Experimentally Induced Pulmonary Lesions: Inhalation Exposure

Species	Monkeys			Rabbits			Guinea Pigs			Rats			Other			Lesions %
Pulmonary Lesions	No.	O	E	No.	O	E	No.	O	E	N	No.	O	E	N	No.	O	E	N
Aerosol Experiments															Ave/Group			
Aluminum	14	16	3	40	17	2	500	125	20		40	7	9		20	27	6	
Silica	20	24	22	60	38		700	540	18	1	126	91	7	1	50	84	2	0.2
Amorphous Silica	18	24	18	146	117	33	680	451	85		330	168	13		80	67	11	
Fibrous Silicates	15	16	12	110	53		610	271	17		240	69	9	2	90	42	4	1
Beryllium	16	24	13	20	18	14	124	44	32	4	1178	679	699	241	50	43	43	10
Miscellaneous A	19	8	2	54	24	5	720	358	38	2	150	90			100	47	5	0.5
Miscellaneous B	15	8	2	80	23		480	218	40	2	100	40			40	43	4	0.4
Miscellaneous C	19	8	6	54	22		480	213	38	2	322	138	34		94	43	7	0.3
SUB-TOTALS	136	128	78	16	2	564	322	54	5	4204	2250	288	11.	2486	1282	771	244	524	207	22	5	49	10	1.5
CONTROLS		64				232				1878				763				230						

FIGURE 13. Histogenesis of adenomatoid carcinoma
- A. Tumor cells arising in respiratory epithelium showing lateral polarity;
- B. Tumor cells spreading over respiratory epithelium;
- C. Tumor cells retaining secretory potential;
- D. Acinus derives by evagination of epithelium;
- E. Acinus is filled with secretory material;
- F. The papilligeroid tumor arises by formation of papilla within epithelialized acinus;
- G. Origin of circinoid histological lesion.

the experimental subjects. In this sense, the human and animal tumors may, therefore, not be strictly comparable. This comparatively brief observation period may also account for the lack of lung tumors in the control animals. The animals that developed tumors were relatively intensely exposed to substances that thereby were proven to be carcinogenic at such dosage levels. Human tumors, on the contrary, arise after much less intense exposure to neoplasiogenic agents. This difference may help to account for the contrasting morphology and topography of human and animal tumors.

Final thought may be given to the possibility of finding an explanation for the diversity of anatomical tumors that were observed in this experimental series, a diversity that also characterizes human lung cancer. Figures 19 and 20 represent schematic explanations or clarifications of these phenomena. The adenomatoid neoplasm may result from dominance of lateral polarity of epithelial cells. It is postulated that each tumor may arise from neoplastic transformation of a single cell with a propensity for lateral division (Fig. 19A), their

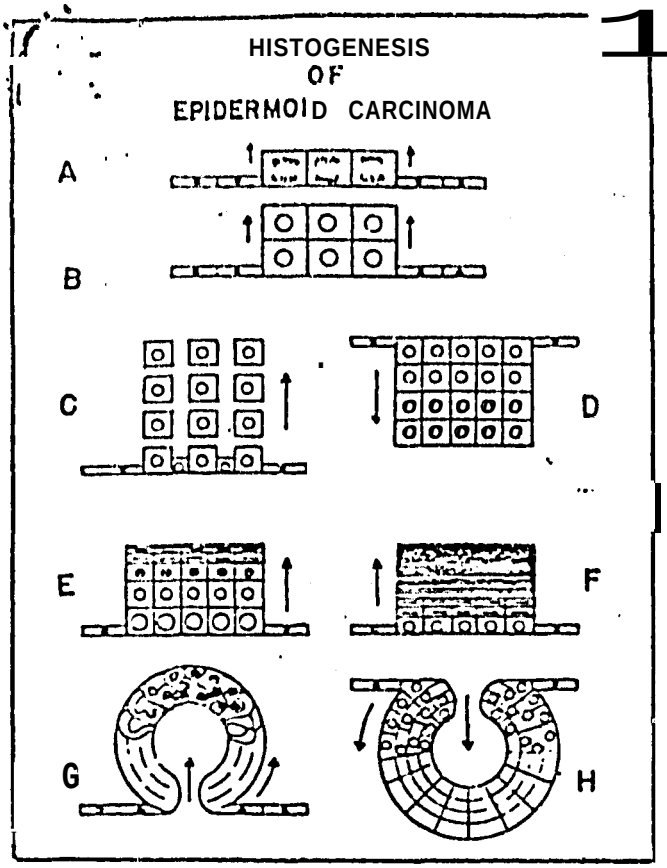

FIGURE 20. Histogenesis of epidermoid carcinoma
A. Neoplastic cells show vertical polarity:
B. Epithelial neoplastic plaque;
C. Desquamative lesion;
D. Granuloma type lesion or invasiveness;
E. Origin of squamoid tumor;
F. Keratinization predominates;
G. Plication of tumor plaque with pseudo-stratified epithelium;
H. Multilayered stratified epithelium lines pseudo-acinus.

daughters perpetuate this trend, and the result will be sheets of neoplastic cells (Fig. 19B and C). If such a sheet evaginates outward, the acinoid histology will result. Such acini may remain empty if the malignant cell is derived from a non-secretory cell (Fig. 19D). If the pre-malignant parent cell is a secretory or goblet cell, the mucigeroid tumor may result (Fig. 19E). If the expanding epithelial sheet buckles inwards, the papilligeroid histology will follow (Fig. 19F). The circinoid lesion may either be an elaboration of a pre-existing papilla or may arise through alternating phases in which lateral and vertical polarity predominate successively (Fig. 19G).

To explain the genesis of the epidermoid carcinoma, it is necessary to postulate dominance of vertical polarity after an initial spurt of lateral polarity which creates a nidus of neoplastic cells (Fig. 20A). The initial effect may be that the plaque of tumor cells (Fig. 20B) creates successive generations of cells which separate or desquamate from the parent cell (Fig. 20C). The cells may also adhere *to* form a multilayered "invasive" epithelium (Fig. 20D). If the surface cells of the latter flatten and manufacture keratin, the squamoid lesion will result (Fig. 20E). Keratinization may be the dominant feature (Fig. 20F). The epithelial plaque may also plicate upwards (Fig. 20G) or downward (Fig. 20H). In the latter case, relatively solid (medullary) lesions may result. The folds of epithelium may become organized as pseudo-stratified or as stratified epithelium.

An explanation why some cells become neoplastic or why only certain of the substances studied proved neoplasiogenic cannot be offered and must await further research. The peculiar atomic lattice of beryllium, which makes it such a valuable metal in nuclear energy physics, may also provide a key to the carcinogenic propensity of this element.

Reprint requests: Industrial Medicine and Surgery, P.O. Box 7151, Fort Lauderdale, Fla. 33304.

Cerrit W. H. Schepers, M.D., D.Sc.